

X-ray analysis of the close binary system FO 15

J.F. Albacete Colombo* and G. Micela

INAF - Osservatorio Astronomico di Palermo, Piazza del Parlamento 1, Palermo, Italy.

Abstract: We analyse the *XMM-Newton* observations of the close massive (O5V((f))+O9.5V) FO 15 binary system. X-ray spectra are described by a combination of absorption models WABS (N_H^{ISM}) and ABSORI (N_H^{wind}) with two absorbed thermal (APEC) models ($kT_1=0.22\pm0.01$ and $kT_2=1.43\pm0.40$ keV) plus a non-thermal Power-Law (PO) model ($\Gamma=1.50\pm0.46$). Observed emission lines from high ionization states of N, O, Ca, Si, Ne and Fe are produced by thermal plasma temperatures according to those obtained from our X-ray spectral fit model. The hard thermal component comes from the colliding wind region (CWR) of the primary stellar wind onto the secondary surface. We find L_x/L_{bol} is about 9.0×10^{-7} in excess with respect to the relation of single O-type stars, likely due to the CWR of the system. We estimate that CWR gas reaches the radiative limit, and mostly emits absorbed soft X-ray photons, while hard X-ray photons come from the inner part of the CWR throughout Inverse Compton (IC) scattering processes. Finally, we confirm the existence of short-term variability which seems to be related to radiative gas at the outer zones of the CWR, since the variability is only present in the soft X-ray band, while the hard X-ray emission remains constant.

1 Introduction

Most of X-ray emission from single O- and early B-type stars display a soft thermal spectrum ($kT\sim0.2-0.9$ keV), as well as an X-ray luminosity (L_x) level approximately scaling with bolometric luminosity (L_{bol}) following a proportionality ratio of $\sim2\times10^{-7}$ (Berghöfer et al. 1997). However, massive binaries often display an additional X-ray luminosity compared to suspected single stars of the same spectral type and luminosity classes (Chlebowski & Garmany 1991). Such an excess is usually attributed to the presence of a colliding wind region (CWR), making the X-ray domain adequate to study the CW phenomena in binary systems. Here we present the X-ray analysis of the close ($P_{orb}=1.41358$ days) massive binary FO 15 (O5V((f)) + O9.5V) (Niemela et al. 2005) of the Carina nebula (NGC 3372).

2 X-ray observations

The Carina Nebula field was observed with *XMM-Newton* in ten separate revolutions. Observations were centered at η Carina or at WR 25 position, leading at the FO 15 positions to off-axis values of 8.45 and 10.1 arcmin, respectively. However, some EPIC observations appear

* e-mail: facundo@astropa.unipa.it

to have CCD gaps and bad columns, that lie close to the centre of the source PSF, yielding unreliable spectral fits. We then performed our spectral analysis using data sets 0112580601 (Rev #115), 0112560101 (Rev.#283) and 0112560301 (Rev,#285). Data were not affected by high level of soft proton background.

3 Spectral analysis

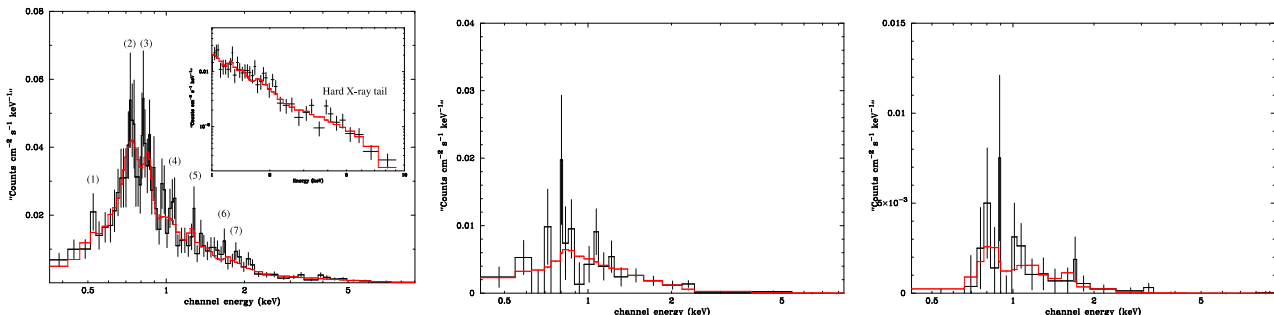
3.1 Getting the spectra

All extracted spectra were acquired in the 0.4 to 10 keV energy range. We use a 30 arcsec radius to extract individual PN and MOS pulse-height source and background spectra, which include almost 90% of the encircled energy by the local PSF. We also constructed the corresponding redistribution matrices (RMF) and ancillary response (ARF) files. The source spectra were binned to reach 2,4 and 9 counts per channel and fit in a simultaneous way to improve the source spectrum statistics.

3.2 Choosing absorption and emission models

In order to obtain the most significant model for the X-ray emission of the FO 15, we choose the Rev.#115, where the source appears brighter.

Figure 1: FO 15 PN spectra from observations in Rev. #115, #283 and #285, respectively.



Note: the solid line shows the best fit model. X-ray emission changes by more than a factor 6 between them, suggesting some kind of phase-locked variability (see discussion in section 3.3). In the left figure we indicate identified emission lines and their identification are presented in an electronic version (see <http://www.astropa.unipa.it/~facundo/proceedings/Table1.pdf>)

We have adopted a “warm” absorber model (Waldron 1984) produced by: *i*) “hot” absorption model related to ionized hydrogen column density stellar wind, and *ii*) “cold” absorption model produced by a neutral hydrogen column, this last fixed at $N_{\text{H}} = 0.62 \times 10^{22} \text{ cm}^{-2}$ (Shull & van Steenberg 1985). We assumed solar abundances throughout our fitting procedures. We first fit single PO as well as single thermal models, in both cases without success. We then tried a 2T thermal model obtaining an overall reduction of the χ^2_{ν} test, but this model was unable to fit data above 3 keV (see Fig. 1-left). As a consequence, we used and adopted a three component model, consisting in two APEC thermal models ($kT_1 = 0.22 \pm 0.01$ and $kT_2 = 1.43 \pm 0.40$ keV) plus another PO component ($\Gamma = 1.50 \pm 0.46$). We discuss the origin of the hard X-ray non-thermal emission in section 3.4.

Absorbed and un-absorbed X-ray fluxes are 1.91×10^{-13} and $15.8 \times 10^{-13} \text{ erg cm}^{-2} \text{ s}^{-1}$ ($L_{\text{x}} =$

$9.5 \times 10^{32} \text{ erg s}^{-1}$ assuming a distance of 2250 pc), giving a luminosity ratio $L_x/L_{\text{bol}} \approx 9.0 \times 10^{-7}$ which is about 4 times greater than accepted estimates for O-type stars.

3.3 X-ray spectral variability

The system has a circular orbit, thus an explanation of the observed X-ray flux variability, such as that observed in Fig 1, is the change of the absorption column density along the line of sight as a function of the orbital phase.

Adopting system and stellar parameters from Niemela et al. (2005), we calculated on-axis momentum balance (η) of the system of 0.05 (see equation 1-left). Then the equal-momentum stagnation point (X_{CWR}^0) is about $14.3 R_{\odot}$, where the total binary separation is only $20 R_{\odot}$, being on-axis primary wind literally shocked onto the secondary photosphere.

Because of the short period of the system ($P=1.41$ days), radiation fields of the companions indeed disturb the acceleration of the winds with the *inhibition effect* (Stevens & Pollock 1994), and/or produces *braking effect* (Gayley et al 1997). Thus, the primary stellar wind ($v_{\text{CWR}}^{\text{wind}}$) at the CWR does not reach velocities greater than 1000 km s^{-1} . The angular component of the stellar wind is at least 370 km s^{-1} , about 40% of the $v_{\text{CWR}}^{\text{wind}}$. Then Coriolis forces result in a substantial distortion of the CWR geometry, being 2D symmetry broken. Furthermore, the off-axis wind-wind collision has smaller v_{\perp} , thus the post shock temperature is lower (between 10^6 to 10^7 K), and the gas is confined to a thermal thin sheet. X-rays emitted from this “thin” region are absorbed by the “cool” wind of the secondary. Following Stevens et al. (1992), we calculated the thermodynamical condition of the gas using equation 1-right.

$$\eta_o = \frac{\dot{M}_2 v_2}{\dot{M}_1 v_1} \qquad \chi_{\text{rad}} = \frac{t_{\text{cool}}}{t_{\text{esc}}} \approx \frac{v_8^4 d_7}{\dot{M}_{-7}} \qquad (1)$$

At the on-axis CWR we found $\chi_{\text{rad}} \approx 0.25$, while off-axis values are even lower $\chi_{\text{rad}} \approx 0.11$. Such radiative CWR successfully explain the observed emission lines (Fig. 1), which require plasmas temperatures between 1.0 to 15 MK. This fact agrees with our two temperature model, where soft emission ($kT_1=0.22$ keV) is produced by instability driven wind shock models of the primary and secondary components, meanwhile hard thermal emission ($kT_2=1.4$ keV) is related to the CWR plasma.

However, our thermal model partially fit some emission lines, being the excesses produced likely by a combination of three effects: *A*) non solar abundances, *B*) non-thermal equilibrium emission lines; and *C*) the intense UV radiation field of O type stars induces a strong enhancement of inter-combination lines (*i*) and decrement of the forbidden (*f*) component (Porquet et al. 2001). Unfortunately, the low resolution of the EPIC spectra makes them unreliable to address these subjects.

3.4 The origin of hard X-ray photons

Thermal hard X-ray photons (energies above 3 keV) are produced in strong wind-wind collisions where the shock compression ratio (χ) is about 4, and the particle energy distribution follows $N(E) \propto E^{-n}$ being $n=(\chi+2)/(\chi-1)=2$ (White & Chen 1995). On the contrary, in close hot massive binaries wind-wind shocks are weaker ($\chi < 4 - n > 2$), producing a steeper particle energy distribution (to lower energies). In hot luminous stars, with thermal plasma greater than 10^7 K ($kT > 0.9$ keV), inverse Compton (IC) cooling becomes more important than collisional cooling, thus reducing the energy available for thermal X-ray emission. Then the competition between

IC losses and shock acceleration processes fix the highest energy of the electrons. In the vicinity of the shock region, as well as near the secondary surface, the magnetic field (B) should not be discarded. Following White & Chen (1995) approximation, and according to wind-photosphere shock velocity of $v_8^{\text{sh}} < 1$ (10^8 cm s^{-1}), a CWR distance from secondary of $r_{\text{AU}} \approx 0.002 \text{ AU}$, a luminosity $L = 10^5 L_{\odot}$ and a typical magnetic field of $B \approx 100 \text{ Gauss}$, we calculated the maximum energy of the electrons at the CWR, *after* IC scattering and *before* IC, which are about 170 MeV and 44 keV, respectively. This difference ($\Delta E_e^{\text{max}} = E_e^{\text{in}} - E_e^{\text{out}}$) is high enough to produce a large relativistic electron population to rise up UV photons ($\sim 0.01 - 0.07 \text{ keV}$) to hard X-ray photons ($> 3.0 \text{ keV}$) by means of IC scattering processes.

4 Short-term variability

We study the existence of short-term variability in FO 15 using the longest observation (Rev. # 115) We extracted background corrected light curves using 4 different bin-sizes of 250, 500, 750 and 1000 sec. The statistical significance of variability were calculated as the ratio of two theoretical χ^2 distributions, that follows the Snedecor F-distribution with $\nu_1 = 1$ and $\nu_2 = N_{\text{bins}} - 2$ degree of freedom. By the fitting of a 4th degree polynomial function we confirm with $P(F_{\chi}) > 95\%$ the existence of variability at time scales of hours, and with amplitude of 25% of the total X-ray emission of FO 15 ($\Delta F_x^0 \sim 3.8 \times 10^{-13} \text{ erg s}^{-1} \text{ cm}^{-2}$).

We also investigate the spectral behavior of short-term variability, and we extracted light-curves for Total- (T_x : 0.2- 10. keV), Soft- (S_x : 0.2-1.2 keV) and Hard- (H_x : 1.2-10.0 keV) energy bands, as well as we compute the hardness ratio of such variability. The observed X-ray variability is dominated mostly by soft X-ray emission ($\sigma / \langle \text{cr} \rangle_{\text{soft}} = 0.35$, while hard energies remain roughly constant ($\sigma / \langle \text{cr} \rangle_{\text{hard}} = 0.21$). Therefore, the observed short-term X-ray variability is related to dynamical instabilities along the CWR, where strong radiative cooling occurs.

Acknowledgments

J.F.A.C acknowledges support by the Marie Curie Fellowship Contract No. MTKD-CT-2004-002769 (*The Influence of Stellar High Energy Radiation on Planetary Atmospheres*).

References

- Berghöfer T., Schmitt J.H.M.M., 1994, Ap&SS, 221, 309
Chen W., 1992, PhD Thesis, Johns Hopkins University
Chlebowski T., Garmany C.D., 1991, ApJ, 368, 241
Gayley K.G., Owocki S.P., Cranmer S.R., 1997, ApJ, 475, 786
Niemela V., Morrell N., Barbá R., Albacete Colombo J.F., Orellana M., 2005, in prep.
O'Toole S.J., Jordan S., Friedrich S., Heber U., 2005, A&A, 437, 227
Porquet D., Mewe R., Raassen A., Kaastra J., Dubau J., 2001, ASPC, 234, 144
Shull J.M., van Steenberg M.E., 1985, AJ, 298, 268
Stevens I.R., Pollock A.M.T., 1994, MNRAS, 269, 226
Waldron W.L., 1984, AJ, 282, 256
White R., Chen W., 1995, IAUS, 163, 438